Research Square

Preprints are preliminary reports that have not undergone peer review.
They should not be considered conclusive, used to inform clinical practice,
or referenced by the media as validated information.

# Antibacterial CM-11 Peptide Potency against the Gram-positive and Gram-negative Bacterial Membrane Models: A Molecular Dynamics Simulations Study

**Reza Mirnejad**
Baqiyatallah University of Medical Sciences
**Mahdi Fasihi-Ramandi**
Baqiyatallah University of Medical Sciences
**Esmaeil Behmard**
Fasa University of Medical Sciences
**Ali Najafi**
Baqiyatallah University of Medical Sciences
**Mehrdad Moosazadeh Moghaddam** ( mm.genetics@gmail.com )
Baqiyatallah University of Medical Sciences

**Research Article**

**Keywords:** Multidrug-resistant bacteria, Cecropin–melittin hybrid peptide, Molecular dynamics simulations

**Posted Date:** March 22nd, 2022

**DOI:** https://doi.org/10.21203/rs.3.rs-1456462/v1

**License:** This work is licensed under a Creative Commons Attribution 4.0 International License.
Read Full License

# Abstract

In the present study, a series of all-atom molecular dynamics simulations were applied to shed light on the molecular mechanism of the activity of CM11, a short cecropin–melittin hybrid peptide obtained through a sequence combination approach, against gram-positive (GP) and gram-negative (GN) bacterial membrane models. In addition, the peptide adsorption mechanism on the surface of the membrane models, the thermodynamic and structural contribution of each residue in the antibacterial activity of the peptide against both GP and GN bacterial membranes were investigated. Our findings showed that the peptide was strongly bound to the GP membrane type in comparison with the GN membrane and was stabilized quickly. These strong bonds are caused by the interactions between basic residues and POPG molecules, which have higher concentrations in GP than GN membranes. Calculation of binding free energies revealed that both electrostatic and van der Waals energy components were desired for the peptide binding and insertion in the membrane. Electrostatic interactions were the main driving force in the adsorption and surface localization of the peptide. Determining the contribution of each residue to the binding free energy indicated that W1, K2, K5, K6 and K9 residues played an important role in the activity of the peptide. These results can be used as a roadmap to provide in-depth insights into the design of appropriate peptides in the fight against multidrug-resistant bacteria.


# 1. Introduction

Over the past decades, beta-lactam antibiotics and glycopeptides such as cefotaxime, imipenem, amoxicillin, cefepime, vancomycin, teicoplanin, telavancin, ramoplanin, decaplanin, corbomycin and complestatin have been used to fight diseases caused by a broad spectrum of gram-positive (GP) and gram-negative (GN) bacteria (Stephens 2020; Blaskovich 2018; Kale-Pradhan 2020). The widespread administration of antibiotics has led to the emergence of resistant bacterial species in human societies (Nathan 2014; Liu 2020). The advent of new pathogenic bacteria has become one of the main threats of human health (Serwecińska 2020; Kumar 2018), as the development of antimicrobial drugs could not adequately help us in the fight against the novel types of infectious diseases ((Stephens 2020). Based on the current rate of antibiotic drugs development, it has recently been estimated that by 2050, more patients will die from bacterial complications than from cancer (Stephens 2020; Kumar 2018). It is also estimated that the costs that this phenomenon will bring to the global health system will exceed $100 trillion (Stephens 2020; Kumar 2018).

Combating such a global crisis requires immediate and coherent action, and alternative antibacterial strategies must be found. One of the new strategies is the use of peptides that have antimicrobial activity (House 2015; Lombardi 2019; Chen 2020). Antimicrobial peptides (AMPs) are amphipathic structures with low molecular weight and a net positive charges of 2 to 9 (Deslouches 2020). Based on the secondary structure, AMPs can be classified into four categories: β-sheet, α-helix, cyclic, and expanded peptides (Koehbach 2019).

The innate immune system in prokaryotes, insects, plants, amphibians, and mammals secretes AMPs in response to external pathogens (Hancock 1999; Zasloff 2002). The function of AMPs varies according to their physicochemical properties and membrane purpose. Studies have shown that the cationic properties of AMPs, conferred by positively charged lysine or arginine residues, play a vital role in their performance (Feng 2015; Jiang 2008; Glukhov 2005). According to most hypotheses concerning the mechanism of antibacterial activity of AMPs, binding of the peptides to target membranes causes changes in membrane permeability, loss of membrane potential, and eventual cell death, although some AMPs have an intracellular target (Bechinger 2017; Lee 2016).

Molecular dynamics (MD) simulations provide a tool to study the structural properties, the dynamic behavior, and the mechanisms of interactions between biomolecules at the atomic level. This method enables us to study carefully the processes involved in the antimicrobial activity of AMPs (Hollingsworth 2018; Farrotti 2015; Huang 2013; Cherniavskyi 2021; Chakraborty 2020). Accordingly, the present study was aimed to implement MD simulations to better understand the membrane-disrupting action of CM11 peptide. The effect of this peptide on mammalian membrane model was also studied to evaluate its non-toxicity. It should be noted that the CM11 peptide is a hybrid peptide derived from N-terminal domain residues of cecropin A (2–8 residues) and hydrophobic C-terminal domain residues of melittin (6–9 residues) with effective antibacterial activity against some of Gram-negative and Gram-positive pathogenic bacteria (Amani 2015).

# 2. Materials And Methods

### 2.1. Peptide structure prediction

PEP-FOLD web-server (Shen 2014), a *de novo* approach for predicting three dimensional model of peptide sequences, was applied to predict the 3D structure of “WKLFKKILKVL” cationic cell penetrating peptide (Figure S1). The server uses a greedy algorithm, driven through a coarse-grained force field for predicting the 3D-structure of input peptides (Shen 2014).

### 2.2 Molecular dynamics simulations

CHARMM-GUI membrane builder was applied to construct membrane bilayer models for bacteria (*S. aureus* and *E. coli*) and mammalian cells (Jo 2008). According to previous studies, GN and GP bacterial membranes comprise a ratio of 3:1 and 1:3 of palmitoyloleoyl-phosphatidylethanolamine (POPE) and palmitoyloleoylphosphatidylglycerol (POPG), respectively [28,29]. To provide the mammalian membrane model, a zwitterionic 1-palmitoyl-2-oleoyl-sn-glycero-3-phosphocholine (POPC) lipid was constructed (Lee 2016; Tsai 2009). The features of all simulation systems are summarized in Table 1.

**Table 1:** Details of all simulations

| Membrane | Lipid composition | Model | Length (ns) |
|---|---|---|---|
| **Gram-positive** | 25% PE, 75% PG | Control | 150 |
| **Gram-positive** | 25% PE, 75% PG | Complex | 300 |
| **Gram-negative** | 75% PE, 25% PG | Control | 150 |
| **Gram-negative** | 75% PE, 25% PG | Complex | 300 |
| **Mammalian** | 100% PC | Control | 150 |
| **Mammalian** | 100% PC | Complex | 300 |

To prepare well equilibrated membranes, each membrane was simulated for 150 ns and the final structure was used as the initial model for the peptide-membrane simulations. The peptide was placed 3 nm away from upper leaflet of the bilayers, after a 100 ns simulation. GROMACS 20.0.4 package was used to perform all MD simulations, using CHARMM36 as the force field (Huang 2013). The TIP3P explicit solvent model was used as the water molecule (Roux 1999). Periodic boundary condition (PBC) was applied in all simulations, and the long-range Coulombic interactions were described by the particle mesh Ewald method (Essmann 1995). The cut-off length for long-range Coulombic and van der Waals bonds was set to 1.2 nm (Van Der Spoel 2005). The LINCS algorithm was used to constrain hydrogen bond lengths of peptide and lipid molecules (Hess 1997). In each system, the protonation state of the peptide was assigned based on calculations at pH 7 (Gordon 2005), and with 0.05 M NaCl. Energy minimization with the steepest descent algorithm was applied for the systems. Each system was then equilibrated for 0.5 ns under a gradual temperature increase to reach 323 K, and then further equilibrated for 2 ns under isothermal-isobaric (NPT) ensemble with the Berendsen weak coupling method (Van Der Spoel 2005). Along the series of equilibration phases, position restraints were applied on lipids and peptide molecules to restrict their motion. Then, the main run was performed for 300 ns without restraints, along which the Nosé-Hoover thermostat and the semi-isotropic Parrinello-Rahman barostat were used to maintain the temperature on 323 K and pressure on 1 bar, respectively (Martyna 1992; Rühle 2008).

### 2.3. Calculation of the free energy of binding

Molecular mechanic Poisson–Boltzmann surface area (MM-PBSA) method was used to calculate the binding free energy between the peptide and the bacterial or mammalian membrane models (Kumari 2014). According to the equation 1, total binding free energy ($\Delta G_{bin}$) is equal to the sum of the different components of polar and non-polar energies:

$$\Delta G_{bin} = \Delta G_{polar} + \Delta G_{nonpolar} \quad (1)$$

The polar term ($\Delta G_{polar}$) is the sum of the components of the electrostatic ($\Delta G_{elec}$) and the polar solvation ($\Delta G_{ps}$) energies:

$\Delta G_{polar} = \Delta G_{elec} + \Delta G_{ps}$ (2)

The non-polar term ($\Delta G_{nonpolar}$) in the equation 1 is the sum of the components of the non-polar solvation ($\Delta G_{nps}$) and the van der Waals ($\Delta G_{vdW}$) energies:

$\Delta G_{nonpolar} = \Delta G_{nps} + \Delta G_{vdW}$ (3)

The total binding free energy of peptide-membrane complexes was computed by g_mmpbsa approach (Kumari 2014), using 100 structures extracted from the last 20 ns of the corresponding simulation trajectory.

# 3. Results And Discussion

### 3.1. Important residues in the peptide activity

To study the mechanism of action of CM11 peptide on bacterial cell membranes and to investigate any differences in the mechanism between GN and GP bacteria, a copy of the peptide model was simulated with each of cell membrane models. Membrane models from *E. coli* and *S. aureus* species were selected to represent pathogenic GN and GP bacterial membranes, respectively. In addition, a copy of the peptide was simulated alongside the eukaryotic membrane model to study the effect of the peptide on the eukaryotic cell membrane.

To clarify the role of the constituting residues in the activities of the peptide against membrane models, radial distribution functions (RDF) between the phosphorus atoms and acyl chains of the bilayer models and polar or nonpolar side chains of residues were calculated, respectively (Fig. 1). The graph for the interaction of K2 with the gram-positive membrane, shows two peaks at 0.3 and 0.4 nm (Fig.1).

These distances represent the establishment of hydrogen bonds and electrostatic interactions between the K2 residue and the membrane phosphorus atom, respectively. Such peaks can also be seen in the RDF graph for K2 in the presence of gram-negative membranes, indicating electrostatic interaction and hydrogen bond (Fig. 1g-h). These results are obviously consistent with experimental studies suggesting that positively-charged residues (R, K) of cationic peptides directly connect with the bacterial membranes (Feng 2015; Jiang 2008; Glukhov 2005; Lee 2016; Tsai 2009).

RDFs between the hydrophobic acyl chains of GP and GN membrane models and the W1 side chain, shown a peak at approximately 0.65 nm, which indicates that hydrophobic interactions are forming between W1 and the acyl chains of GP and GN membranes (Figure S1e-f and Fig 1g-h). Generally, these results indicate the penetration of hydrophobic side chains into the membrane to interact with the hydrophobic tail of bacterial membrane models (Figure S1e-f and Fig 1g-h).

### 3.2. Selectivity for bacterial membrane

To address the peptide activity against both GP and GN bacteria without mammalian cytotoxicity, the adsorption mechanism of the peptide on the surface of GP, GN, and mammalian membranes was investigated. The distances between the center of mass (COM) of the membranes and that of the peptide molecule were measured as a function of time (Fig. 2a).

There are high fluctuations in the graph of the distance between the peptide and the mammalian membrane, indicating the instability of the interaction between the peptide and the membrane. This implies the reluctance of the peptide to bind to the surface of the mammalian membrane, probably due to the presence of the amino group in the polar heads of POPC lipid. The positive charge of $-NH_3$ groups can disrupt the interaction between the cationic peptide and the membrane. This result is consistent with previous studies (Lee 2016). Figure 2a-d also shows that the peptide interacts with both GN and GP bacterial membranes. Though, the peptide molecule is closer to COM of the GP membrane than to COM of the GN membrane. This difference could be due to the effect of the peptide or a change in the membrane thickness. Therefore, changes in the membrane thickness (Fig. 2b, Table 2) and the peptide adsorption depth were calculated (Table 2).

**Table 2:** Thickness of the bilayer membranes and the adsorption depth for the peptide molecule

| Bilayer | Model | Bilayer thickness (nm) | Adsorption depth |
|---|---|---|---|
| **Gram-positive** | Control | 3.62 | N/A |
| **Gram-positive** | Complex | 3.82 | 0.16 |
| **Gram-negative** | Control | 3.87 | N/A |
| **Gram-negative** | Complex | 4.04 | 0.3 |

The distance between phosphate groups on the two sides of the bilayer membrane was considered as the membrane thickness, and the adsorption depth was obtained by calculating the gap between phosphates in the upper leaflet with the peptide molecule. These analyzes showed that the gram-negative bacterial membrane was thicker than the gram-positive bacterial membrane. It was also found that the distance between top phosphate and the peptide for gram-negative membrane is 0.3 nm and this distance for gram-positive bacteria is 0.16 nm. Accordingly, the peptide binds more deeply to the gram-positive bacterial membrane. This difference may be due to the higher concentration of POPG molecules in this membrane than the gram-negative membrane.

To reveal the contribution of components of the energies in the peptides' binding process, the interaction energies between the peptide and bacterial lipids were analyzed in terms of separate electrostatic and van der Waals (vdW) components (Fig. 2c). The electrostatic component has a much greater share than vdW in the binding process during the penetration of the peptide. In general, the GP-peptide interaction was slightly more favorable than the GN-peptide interaction. Concordantly, the total number of contacts formed between the peptide and GP (Fig. 2d) increases sharply at about 215000 ps time point of the simulation. The number of bonds between GP and the peptide is higher than that for the peptide-GN and

demonstrates a higher slope with time, which indicates a high affinity and membrane Permeability of Peptide for GP.

### 3.3. Disruption of bacterial membrane induced by peptide

To better understand the activity of the peptide against all three types of membrane models studied, the gmx_order tool was used to calculate the average deuterium order parameter ($S_{CD}$). The $S_{CD}$ parameter was calculated by solving the equation 4. In this equation, θ indicates the angle between the membrane normal and the C-D bond vector. Also, the brackets is an average over all equivalent POPC, POPE and POPG molecules during the simulations.

$$S_{CD} = \left\langle \frac{3\cos 2\theta - 1}{2} \right\rangle \quad (4)$$

A higher value $S_{CD}$ in the pure membrane than the peptide-membrane complex indicates that the order of the acyl chains is disturbed by the peptide. Analysis of $S_{CD}$ parameter in this study showed that the interactions between membranes and the peptide lead to decrease in the ordering of acyl chains compared to pure membranes (Fig. 3).

### 3.4. Driving forces

To determine the role of each of the energy components as well as to better understand the interactions between the peptide and the membrane, the binding free energies of the peptide-bilayer complexes were analyzed by MM-PBSA approach. As listed in Table 3, polar and non-polar interactions are the energy components desired for the peptide's binding to bacterial membrane models.

**Table 3:** The share of each energy component in the binding free energy ($\Delta G_{bin}$; kJ/mol)

| Energy components | GP | GN | Mammalian |
|---|---|---|---|
| $\Delta E_{ele}$[a] | -8711.031±716.468 | -3394.680±309.278 | 50.479± 34.188 |
| $\Delta E_{vdW}$[b] | -187.373±52.566 | -121.148± 38.771 | -0.204±0.531 |
| ΔGsol-ele[c] | 1332.122±448.569 | 873.548±271.662 | 31.331±82.507 |
| ΔGsol-np[d] | -7.981±6.705 | -22.139±5.026 | 0.315±2.360 |
| $\Delta E_{non\text{-}polar}$[e] | -195.354±29.64 | −143.287±21.89 | 0.111±1.45 |
| $\Delta E_{polar}$[f] | -7378.909±582.517 | -2521.132±290.47 | 81.81±58.347 |
| $\Delta G_{bind}$[g] | -7574.263±302.57 | −2664.419±155.81 | 81.921±29.89 |

[a]Electrostatic energy, [b]van der Waals energy, [c]Polar solvation energy, [d]Non-polar- solvation, The computed binding free energy and the contribution of diverse energy elements (kJ/mol). [a]Electrostatic energy, [b]van der Waals energy, [c]Polar solvation energy, [d]Non-polar- solvation energy, [e]Non-polar connection, [f]Polar connection, [g]Binding free energy.

The role of polar interactions is more significant, thus, polar interactions can be known as the main driving force in the binding process. Our results indicate that electrostatic interactions play a key role in the membrane surface binding process, and hydrophobic energies play a role in the process of peptide insertion in the membrane. These results are well consistent with previous studies (Feng 2015; Jiang 2008; Glukhov 2005; Lee 2016).

According to Table 3, the binding free energy ($\Delta G_{bin}$) calculated for the GP-peptide complex is approximately three times greater than that for the GN-peptide complex. This large difference is due to polar interactions, especially electrostatic interactions. The different composition of lipid molecules that form the bacterial membranes of GN and GP causes such a sharp difference. The number of PG molecules in GP bacterial membrane is much higher than that in the GN types. If it is assumed that the antibacterial activity of the peptide is directly related to the strength of the interactions between the peptide and the membrane, our finding is consistent with observations that show that cationic peptides have stronger antibacterial effects against GP than GN bacterial species (Feng 2015; Jiang 2008; Glukhov 2005; Lee 2016). In addition, to determine the contribution of each residue in the $\Delta G_{bin}$, the free energy decomposition of each residue was calculated. Figure 4a-c shows that K2, K5, K6 and K9 have a greater share in the peptide binding free energy to both GP and GN bacterial membranes. Consistently, previous studies have demonstrated that basic residues are essential in the interaction of cationic peptides with bacterial membranes (Feng 2015; Jiang 2008; Glukhov 2005; Lee 2016).

Our results show that each of these residues has a multiplier contribution in binding of the peptide to the GP type of bacterial membrane compared to the GN type. Among the basic residues, K2 and K5 have the largest share in the $\Delta G_{bin}$. This indicates the important role of these residues in the antibacterial activity of the peptide. The importance of hydrophobic interactions in the binding process and penetration of antibacterial peptides has been reported (Feng 2015; Jiang 2008; Glukhov 2005; Lee 2016). In the simulation of GP and GN membranes, the residue W1 created effective hydrophobic interactions with the membrane models, indicating the possible involvement of W1 in the antibacterial activity of the peptide.

The $\Delta G_{bin}$ of the mammalian-peptide was positive. This result indicates the reluctance of the studied peptide to bind to the mammalian membrane model. The presence of positively charged amino groups in the polar heads of the POPC lipid molecules could be the main reason for the unfavorable binding of the cationic peptide to this membrane model.

### 3.4.2 Partial density of all atoms in the membrane models

To better understand and validate the effect of the peptide on the structure and coherence of membrane models, the partial density of atoms across the bilayer membrane was calculated. According to Figure 4, the density profile of the peptide almost completely overlaps with the region corresponding to the density of the polar head groups. This indicates the surface localization of the peptide on the bacterial membrane models. The peptide is located deeper in the GP than in the GN bacterial membrane. In addition, the density profiles of the studied membrane models clearly show that, compared to other membrane models, the peptide is inserted more deeply into the hydrophobic tails of the GP membrane. These results are well consistent with the other analyzes performed in this study.

# 4. Conclusion

This study was aimed to elucidate the adsorption of CM11 as an AMP molecule on bacterial and mammalian membranes in terms of its displacement relative to the membrane center. Our simulation results showed that the peptide was clearly adsorbed to the membrane surface of both GP and GN types of bacteria. But it is never permanently adsorbed on the surface of the mammalian membrane. It was also found that the binding of the peptide to the surface of the GP bacterial membrane is much stronger than its binding to the GN bacterial membrane. This is due to the high concentration of POPG lipid molecules in GP compared to GN. On the other hand, it was found that polar interactions caused by basic residues play an important role in the process of peptide adsorption and surfacelocalization on the bacterial membrane. The present study illuminates the thermodynamic and structural basis of the peptide's antibacterial activity against GN and GP membranes and provides a useful understanding of the design of strong AMPs to be used against resistant bacteria.

# Declarations

### Additional Information

Supplementary information accompanies this paper, including Supplementary Figure S1.

**Acknowledgements: none**

**Author contribution:**

RM and MFR contributed to resource and funding acquisition. EB conceptualized the work and completed the draft performed data curation, analysis, validation, and visualization; and wrote the original draft. AN contributed to project administration. MMM contributed to project administration, resources, and funding acquisition. All authors reviewed the final manuscript. **Funding: none**

**Availability of data and material:** No datasets were generated or analysed during the current study. All data generated or analysed during this study are included in this published article and its Supplementary Information files.

- **Conflict of interest:** The authors declare no competing interests.

# References


1. Amani J, Barjini A, Moghaddam KM, Asadi A (2015) In vitro synergistic effect of the CM11 antimicrobial peptide in combination with common antibiotics against clinical isolates of six species of multidrug-resistant pathogenic bacteria. Protein Pept Lett 22(10):940–951. https://doi.org/10.2174/0929866522666150728115439
2. Bechinger B, Gorr SU (2017) Antimicrobial peptides: mechanisms of action and resistance. J Dent Res 96(3):254–260. https://doi.org/10.1177/0022034516679973
3. Blaskovich MA, Hansford KA, Butler MS, Jia Z, Mark AE, Cooper MA (2018) Developments in glycopeptide antibiotics. ACS Infect Dis 4(5):715–735. https://doi.org/10.1021/acsinfecdis.7b00258
4. Chakraborty A, Kobzev E, Chan J, de Zoysa GH, Sarojini V, Piggot TJ, Allison JR (2020) Molecular dynamics simulation of the interaction of two linear battacin analogs with model Gram-positive and Gram-negative bacterial cell membranes. ACS omega 6(1):388–400. https://doi.org/10.1021/acsomega.0c04752
5. Chen CH, Lu TK (2020) Development and challenges of antimicrobial peptides for therapeutic applications. Antibiotics 9(1):24. https://doi.org/10.3390/antibiotics9010024
6. Cherniavskyi YK, Oliva R, Stellato M, Del Vecchio P, Galdiero S, Falanga A, Tieleman DP (2021) Structural characterization of the antimicrobial peptides myxinidin and WMR in bacterial membrane mimetic micelles and bicelles. https://doi.org/10.1101/2021.03.30.437760. bioRxiv
7. Deslouches B, Montelaro RC, Urish KL, Di YP (2020) Engineered cationic antimicrobial peptides (eCAPs) to combat multidrug-resistant bacteria. Pharmaceutics 12(6):501. https://doi.org/10.3390/pharmaceutics12060501
8. Essmann U, Perera L, Berkowitz ML, Darden T, Lee H, Pedersen LG (1995) A smooth particle mesh Ewald method. J Chem Phys 103(19):8577–8593. https://doi.org/10.1063/1.470117
9. Farrotti A, Bocchinfuso G, Palleschi A, Rosato N, Salnikov ES, Voievoda N, Stella L (2015) Molecular dynamics methods to predict peptide locations in membranes: LAH4 as a stringent test case. Biochim et Biophys Acta (BBA)-Biomembranes 1848(2):581–592. https://doi.org/10.1016/j.bbamem.2014.11.002
10. Feng Q, Huang Y, Chen M, Li G, Chen Y (2015) Functional synergy of α-helical antimicrobial peptides and traditional antibiotics against Gram-negative and Gram-positive bacteria in vitro and in vivo. Eur J Clin Microbiol Infect Dis 34(1):197–204. https://doi.org/10.1007/s10096-014-2219-3
11. Glukhov E, Stark M, Burrows LL, Deber CM (2005) Basis for selectivity of cationic antimicrobial peptides for bacterial versus mammalian membranes. J Biol Chem 280(40):33960–33967. https://doi.org/10.1074/jbc.M507042200
12. Gordon JC, Myers JB, Folta T, Shoja V, Heath LS, Onufriev A (2005) H++: a server for estimating p K as and adding missing hydrogens to macromolecules. Nucleic Acids Res 33(suppl2):W368–W371.

https://doi.org/10.1093/nar/gki464

13. Hancock RE, Chapple DS (1999) Peptide antibiotics. Antimicrob Agents Chemother 43(6):1317–1323. https://doi.org/10.1128/AAC.43.6.1317
14. Hess B, Bekker H, Berendsen HJ, Fraaije JG (1997) LINCS: a linear constraint solver for molecular simulations. J Comput Chem 18(12):1463–1472
15. Hollingsworth SA, Dror RO (2018) Molecular dynamics simulation for all. Neuron 99(6):1129–1143. https://doi.org/10.1002/(SICI)1096-987X(199709)18:12%3C1463::AID-JCC4%3E3.0.CO;2-H
16. House W (2015) National action plan for combating antibiotic-resistant bacteria. The White House, Washington, DC
17. Huang J, MacKerell AD Jr (2013) CHARMM36 all-atom additive protein force field: Validation based on comparison to NMR data. J Comput Chem 34(25):2135–2145. https://doi.org/10.1002/jcc.23354
18. Huang K, García AE (2013) Free energy of translocating an arginine-rich cell-penetrating peptide across a lipid bilayer suggests pore formation. Biophys J 104(2):412–420. https://doi.org/10.1016/j.bpj.2012.10.027
19. Jiang Z, Vasil AI, Hale JD, Hancock RE, Vasil ML, Hodges RS (2008) Effects of net charge and the number of positively charged residues on the biological activity of amphipathic α-helical cationic antimicrobial peptides. Pept Sci 90(3):369–383. https://doi.org/10.1002/bip.20911
20. Jo S, Kim T, Iyer VG, Im W (2008) CHARMM-GUI: a web-based graphical user interface for CHARMM. J Comput Chem 29(11):1859–1865. https://doi.org/10.1002/jcc.20945
21. Kale-Pradhan PB, Giuliano C, Jongekrijg A, Rybak MJ (2020) Combination of Vancomycin or Daptomycin and Beta-lactam Antibiotics: A Metaanalysis. Pharmacotherapy: The Journal of Human Pharmacology and Drug Therapy 40(7):648–658. https://doi.org/10.1002/phar.2437
22. Koehbach J, Craik DJ (2019) The vast structural diversity of antimicrobial peptides. Trends Pharmacol Sci 40(7):517–528. https://doi.org/10.1016/j.tips.2019.04.012
23. Kumar A, Pal D (2018) Antibiotic resistance and wastewater: correlation, impact and critical human health challenges. J Environ Chem Eng 6(1):52–58. https://doi.org/10.1016/j.jece.2017.11.059
24. Kumari R, Kumar R, Open Source Drug Discovery Consortium, &, Lynn A (2014) g_mmpbsa: A GROMACS tool for high-throughput MM-PBSA calculations. J Chem Inf Model 54(7):1951–1962. https://doi.org/10.1021/ci500020m
25. Lee J, Jung SW, Cho AE (2016) Molecular insights into the adsorption mechanism of human β-defensin-3 on bacterial membranes. Langmuir 32(7):1782–1790. https://doi.org/10.1021/acs.langmuir.5b04113
26. Lee TH, Hall N, Aguilar MI (2016) Antimicrobial peptide structure and mechanism of action: a focus on the role of membrane structure. Curr Top Med Chem 16(1):25–39
27. Liu J, Gefen O, Ronin I, Bar-Meir M, Balaban NQ (2020) Effect of tolerance on the evolution of antibiotic resistance under drug combinations. Science 367(6474):200–204. https://doi.org/10.1126/science.aay3041

28. Lombardi L, Falanga A, Del Genio V, Galdiero S (2019) A new hope: self-assembling peptides with antimicrobial activity. Pharmaceutics 11(4):166. https://doi.org/10.3390/pharmaceutics11040166
29. Martyna GJ, Klein ML, Tuckerman M (1992) Nosé–Hoover chains: The canonical ensemble via continuous dynamics. J Chem Phys 97(4):2635–2643. https://doi.org/10.1063/1.463940
30. Nathan C, Cars O (2014) Antibiotic resistance-problems, progress, and prospects. N Engl J Med 371(19):1761–1763
31. Roux B, Simonson T (1999) Implicit solvent models. Biophys Chem 78(1–2):1–20
32. Rühle V (2008) Pressure coupling/barostats. J Club. https://doi.org/10.1016/S0301-4622(98)00226-9
33. Serwecińska L (2020) Antimicrobials and Antibiotic-Resistant Bacteria: A Risk to the Environment and to Public Health. Water 12(12):3313. https://doi.org/10.3390/w12123313
34. Shen Y, Maupetit J, Derreumaux P, Tufféry P (2014) Improved PEP-FOLD approach for peptide and miniprotein structure prediction. J Chem Theory Comput 10(10):4745–4758. https://doi.org/10.1021/ct500592m
35. Stephens LJ, Werrett MV, Sedgwick AC, Bull SD, Andrews PC (2020) Antimicrobial innovation: a current update and perspective on the antibiotic drug development pipeline. Future Med Chem 12(22):2035–2065. https://doi.org/10.4155/fmc-2020-0225
36. Tsai CW, Hsu NY, Wang CH, Lu CY, Chang Y, Tsai HHG, Ruaan RC (2009) Coupling molecular dynamics simulations with experiments for the rational design of indolicidin-analogous antimicrobial peptides. J Mol Biol 392(3):837–854. https://doi.org/10.1016/j.jmb.2009.06.071
37. Van Der Spoel D, Lindahl E, Hess B, Groenhof G, Mark AE, Berendsen HJ (2005) GROMACS: fast, flexible, and free. J Comput Chem 26(16):1701–1718. https://doi.org/10.1002/jcc.20291
38. Zasloff M (2002) Antimicrobial peptides of multicellular organisms. Nature 415(6870):389–395. https://doi.org/10.1038/415389a

# Figures

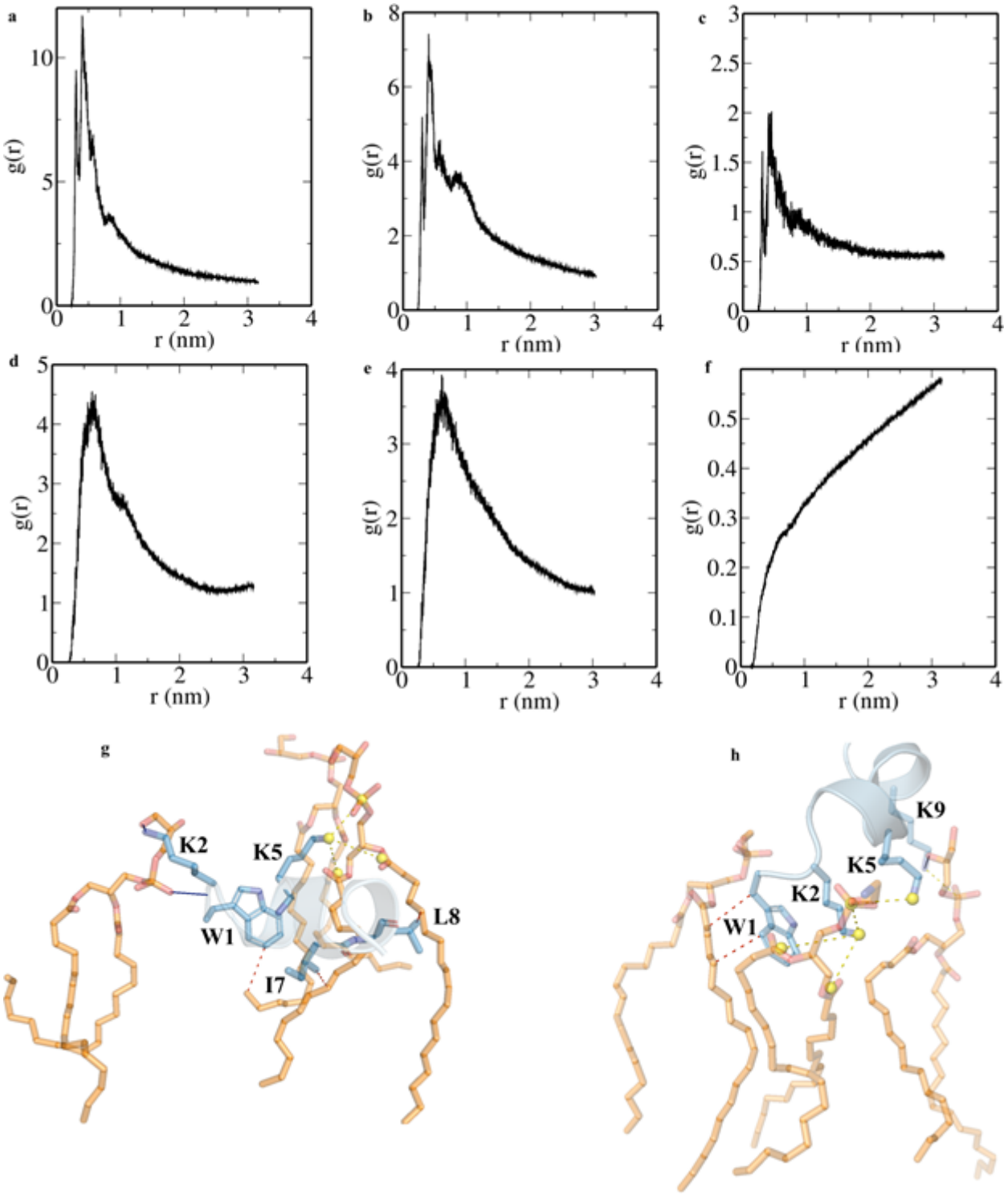


## Figure 1

The RDF graphs between the side chain of K2 and the phosphorus atoms of GP, GN and mammalian model bilayers, respectively (a-c), and the graphs between the side chain of W1 and the acyl chains of GP, GN and mammalian model bilayers, respectively (d-f). Interactions between the lipid molecules (wheat sticks), (g (GN), h (GP)), and the main residues (blue sticks mode) of the peptide (light blue cartoon). Hydrophobic interactions highlighted in red dashed line, saltbridges highlighted in yellow dashed line and hydrogen bond highlighted in blue line.

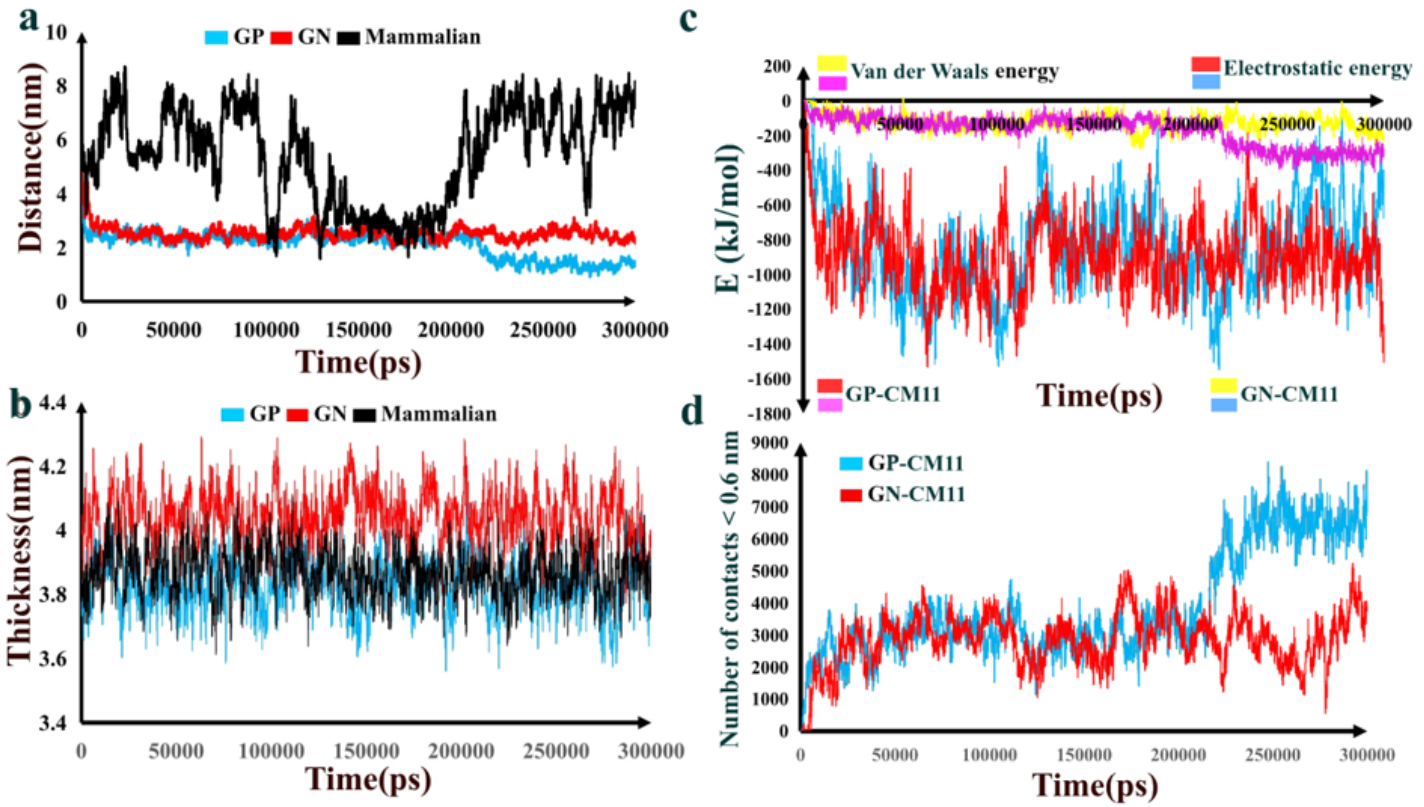


## Figure 2

Distance between center of mass (COM) of the peptide (CM11) and COM of the mammalian and bacterial membranes (a). Bacterial and mammalian membrane thickness (distance between upper and down phosphorus atoms) along the simulation times (b). The interaction energies between the CM11 and bacterial membrane (c). The number of contacts between the CM11 and the bacterial membrane (d).

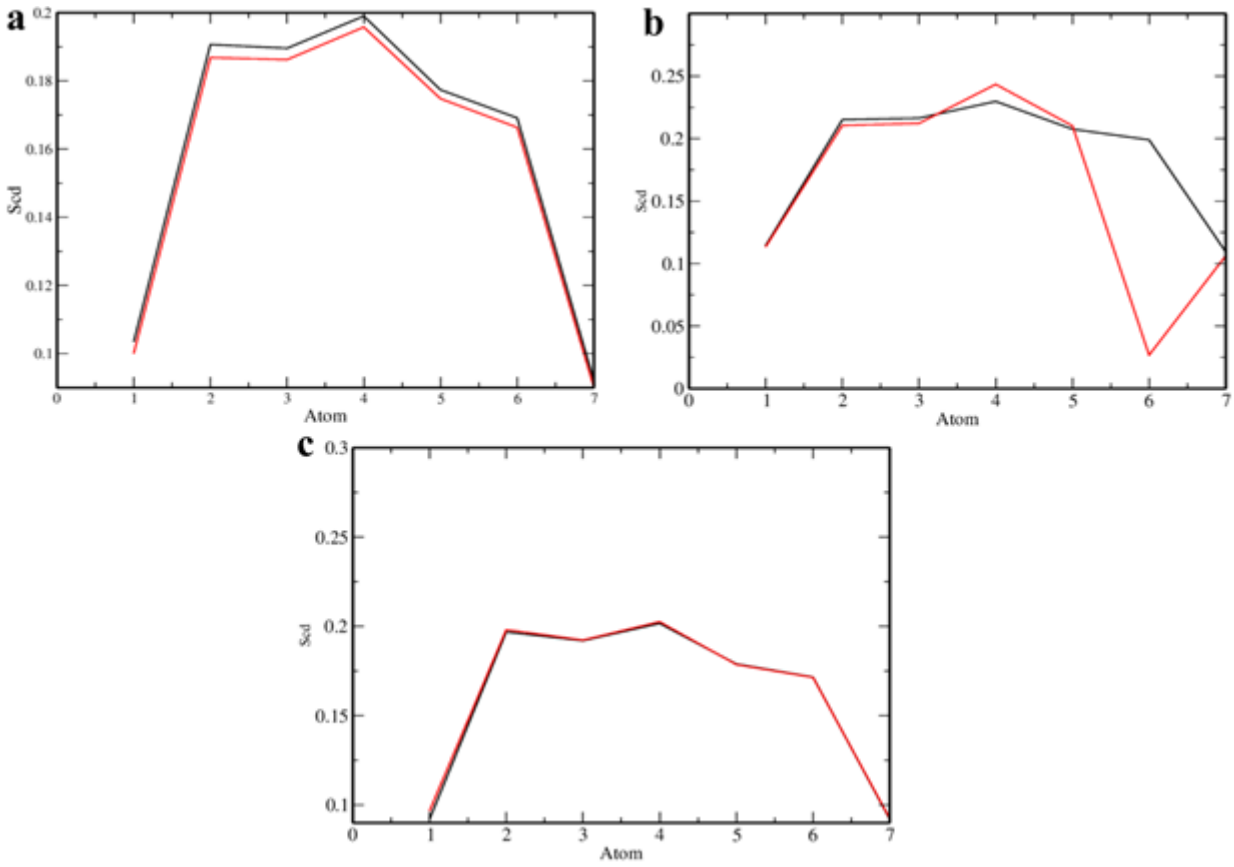


## Figure 3

Order parameters of the nonpolar tails of GP (a), GN (b), and mammalian (c), membranes in the presence (red line), and absence (black line), of the peptide.

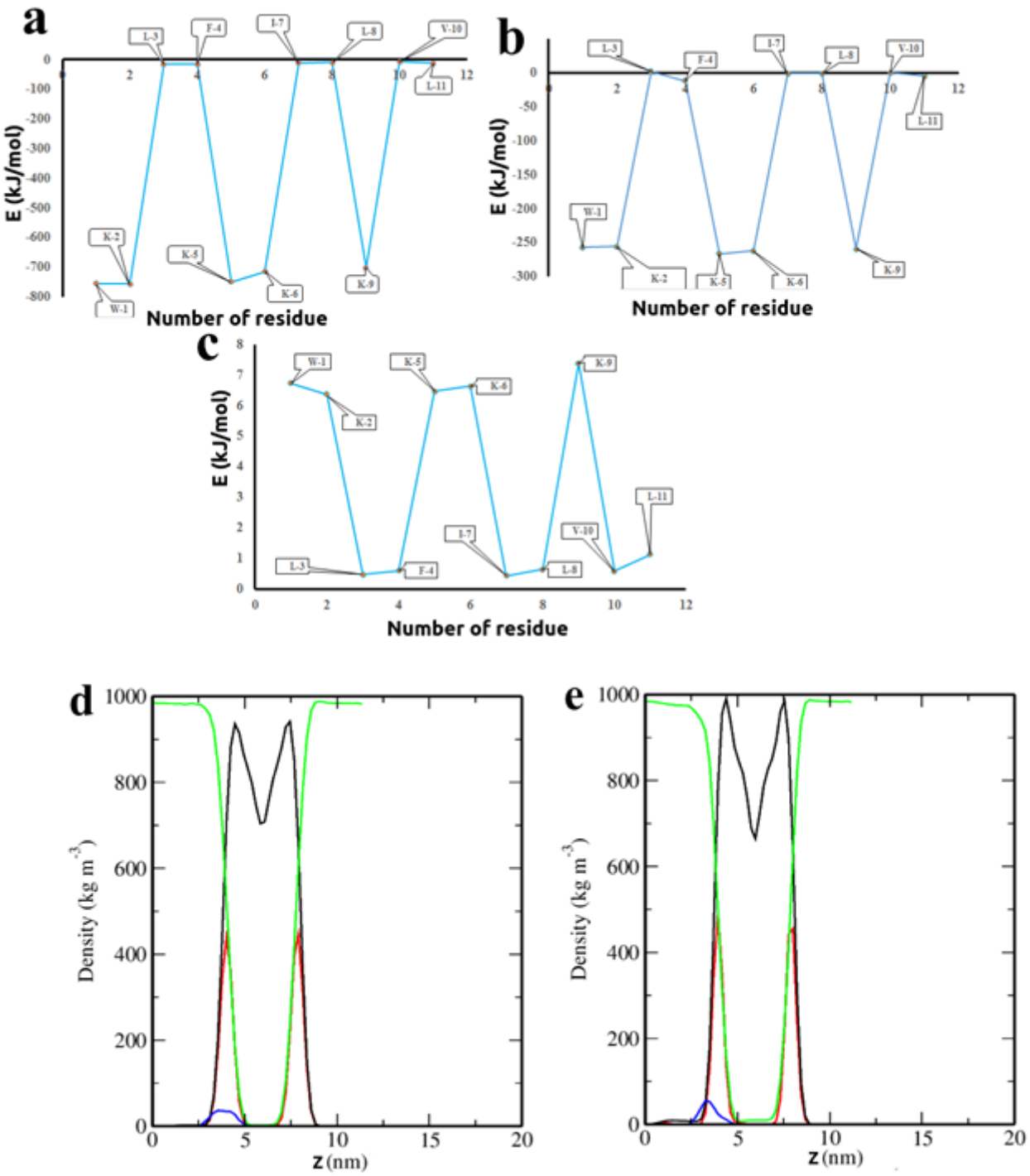


**Figure 4**

Contribution of the peptide residues to the binding free energy in the GP-peptide (a), GN-peptide (b) and mammalian membrane-peptide (c) complexes. Partial density plots of the polar head groups (red line), bilayer molecules (black line), water molecules (green line), and the peptide molecule (blue line), during simulation of GP (d), and GN (e), bacterial membranes.

# Supplementary Files

This is a list of supplementary files associated with this preprint. Click to download.

- supplementaryinformation.docx